

Effect of Ni Additions on the Microstructure, Mechanical Properties, and Electrical Conductivity of Al Alloy

Hyo-Sang Yoo, Yong-Ho Kim, Cheol-Woo Kim, Se-Weon Choi, and Hyeon-Taek Son[†]

Korea Institute of Industrial Technology, Republic of Korea

(Received September 17, 2021 : Revised November 9, 2021 : Accepted December 6, 2021)

Abstract In this paper, the effect of Ni (0, 0.5 and 1.0 wt%) additions on the microstructure, mechanical properties and electrical conductivity of cast and extruded Al-MM-Sb alloy is studied using field emission scanning electron microscopy, and a universal tensile testing machine. Molten aluminum alloy is maintained at 750 °C and then poured into a mold at 200 °C. Aluminum alloys are hot-extruded into a rod that is 12 mm in diameter with a reduction ratio of 39:1 at 550 °C. The addition of Ni results in the formation of Al₁₁RE₃, AlSb and Al₃Ni intermetallic compounds; the area fraction of these intermetallic compounds increases with increasing Ni contents. As the amount of Ni increases, the average grain sizes of the extruded Al alloy decrease to 1359, 536, and 153 μm, and the high-angle grain boundary fractions increase to 8, 20, and 34 %. As the Ni content increases from 0 to 1.0 wt%, the electrical conductivity is not significantly different, with values from 57.4 to 57.1 % IACS.

Key words aluminum, nickel, extrusion, mechanical property, electrical conductivity.

1. Introduction

Recently, research on improving the heat dissipation characteristics of products has actively been conducted in accordance with the trend of high integration, high output and energy saving of electric conductors, transmission lines, communication cables, motors, and LEDs. Aluminum and its alloys have been extensively applied in the electric power industry because of their excellent conductivity, low cost, good formability and lightweight properties. In addition, aluminum is widely used throughout the industry owing to its high corrosion resistance and weldability.¹⁻³⁾ In the case of electrical products, if the heat dissipation characteristics cannot be secured, the efficiency and service life rapidly deteriorate, so heat dissipation performance is required for high output. However, the addition of other elements to pure aluminum lowers the conductivity owing to solute atoms, grain boundaries, dislocations, and deposits. The most important effect on the reduction in electrical conductivity occurs in the solute atoms. In other words, high strength is always incompatible with the high electrical conductivity of metallic materials. Recently, much research has been conducted to increase the strength of Al alloys and lower their electrical resistance.⁴⁻⁷⁾

Al-based immiscible systems such as Al-RE are considered to be promising materials for high conductors because they have zero solubility in Al and have little effect on electrical conductivity. Compared to solid solutions, intermetallic compounds do not significantly affect the electrical conductivity because they do not significantly deform the crystal structure of the metal. In addition, the uniform distribution of small intermetallic compounds throughout the alloy can significantly increase the mechanical strength and thermal stability. However, control is necessary because excessive amounts of immiscible element compounds can cause loss of electrical conductivity.^{8,9)} Recently, numerous studies on rare earth (RE) related to the properties of Al alloys have been conducted, and it has been shown that RE alloys have great potential for changes in their microstructure and properties. However, Al-RE alloys are stronger than pure aluminum, but still lack strength, owing to the large particles of intermetallic compounds. Among rare earth metals, misch metal (MM) has been reported to have modifier in Al alloys. It has been found that La or Ce can act as a modifier in Al alloys to improve the shape of eutectic particles and thus the tensile strength.^{10,11)}

The microstructure of the alloy is determined by the

[†]Corresponding author

E-Mail : sht50@kitech.re.kr (H.-T. Son, KITECH)

© Materials Research Society of Korea, All rights reserved.

This is an Open-Access article distributed under the terms of the Creative Commons Attribution Non-Commercial License (<http://creativecommons.org/licenses/by-nc/3.0>) which permits unrestricted non-commercial use, distribution, and reproduction in any medium, provided the original work is properly cited.

overall composition, and the phase composition could be changed by adding modifiers. In Al alloys, Bi, Sr, Sc and Sb elements have been reported to be good modifiers. Among them, Sb can not only refine the phase through the adsorption poisoning effect of additive elements, but also form a fine process phase. In addition, Sb has a stable modification effect and excellent casting properties.¹²⁾ In general, transition metals(TM) are used as additives in aluminum-based alloys. Unique properties were observed when nickel was added to a crystalline Al-based alloys. The eutectic reaction of Ni and Al can generate high-temperature stable Al₃Ni intermetallic phase to obtain high-temperature stability in the composite. Ni-added alloys produced by rapid solidification are being studied extensively due to their unique structure, properties and potential industrial applications. The addition of Ni is being studied as a material that can increase castability without affecting conductivity.^{13,14)}

In this study, we investigated the effect of the addition of Ni on the microstructure, mechanical properties, and electrical conductivity of as-cast and as-extruded Al-MM-Sb alloys.

2. Experimental Procedure

The alloys used in this study had the nominal composition of Al-1.5 wt%MM-1.5 wt%Sb-xNi alloys ($x = 0, 0.5$ and 1.0 wt%). The melt was held at $750\text{ }^{\circ}\text{C}$ for 20 min and then poured into a pre-heated steel mold (diameter = 75 mm, height = 250 mm) at $200\text{ }^{\circ}\text{C}$. The cast alloys were machined into billets with a diameter of 70 mm and a height of 90 mm. The machined billets were homogenized at $570\text{ }^{\circ}\text{C}$ for 4 h. The billets were

hot extruded into rod that were 12 mm in diameter with a reduction ratio of 38:1 at $550\text{ }^{\circ}\text{C}$. In order to observe their microstructures, the specimens were polished with a diamond suspension of $3\text{ }\mu\text{m}$ and $1\text{ }\mu\text{m}$, and then silica suspension was used for the fine polishing. For EBSD analysis, electrolytic polishing was performed in a solution using 2 % butylcellosolve, 8 % HClO₄, 30 % alcohol and 60 % water. The microstructures of the alloys were examined using a field emission scanning electron microscopy (FE-SEM) and electron backscatter diffraction (EBSD) system. The phase composition of the alloys was examined using a scanning electron microscope equipped with an energy-dispersive X-ray spectrometer (EDS) and X-ray diffractometer (XRD) with Cu K α radiation. The electric conductivities of the alloys were measured using the eddy current method at room temperature. The mechanical properties of the as-extruded Al alloy specimens were measured by universal testing machine with ASTM E8M standard. Tensile tests were carried out at an initial strain rate of $1.0 \times 10^{-3}\text{ s}^{-1}$.

3. Results and Discussion

Fig. 1 shows the SEM-BSE images of the as-cast and as-extruded of Al-1.5 wt%MM-1.5 wt%Sb-xNi ($x = 0, 0.5$, and 1.0 wt%) alloys. As can be seen from the as-cast microstructure in Fig. 1[(a)-(c)], the FCC-Al matrix has a black contrast, and intermetallic compounds have a gray and white contrast at the grain boundaries. The microstructures of the gray and white parts are rather simple and composed of lamellar white and small needle-like and angular-shaped gray parts. The intermetallic compounds fraction according to the amount of Ni added to

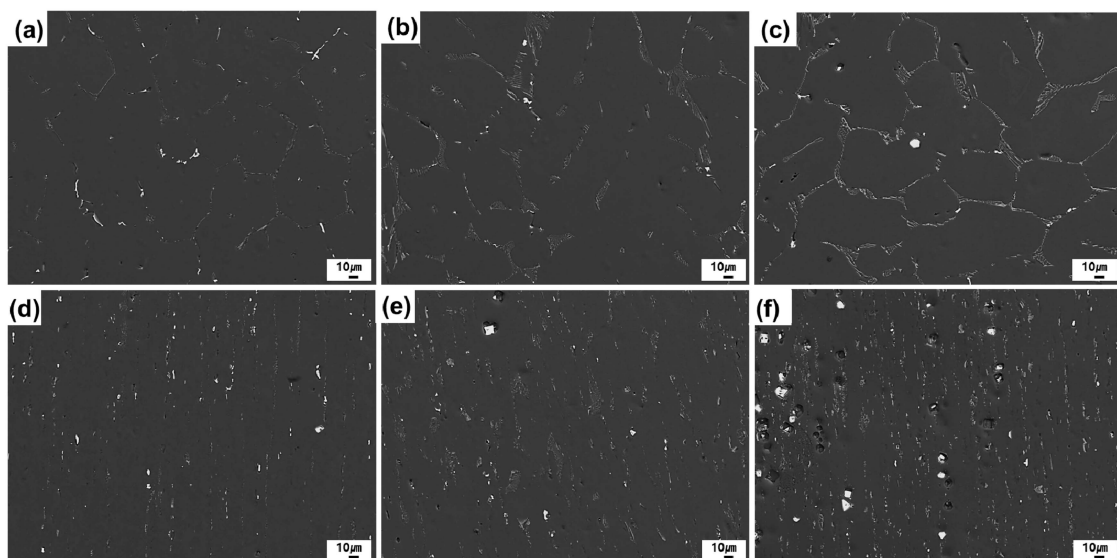


Fig. 1. SEM images of the as-cast (a to c) and as-extruded (d to f) Al-1.5 wt%MM-1.5 wt%Sb-xNi alloys [$x = 0$ (a, d), 0.5 (b, e) and 1.0 wt% (c, f)].

the as-cast Al-MM-Sb alloy was investigated using an image analyzer. The volume fraction of 2nd phases in the Al-1.5wt%MM-1.5wt%Sb alloy were 98.6 and 1.42 %, respectively. As the Ni content increased from 0 to 1.0 wt%, the intermetallic fraction increased to 1.4, 3.3 and 5.5 %. According to Polmear et al., study, the shape and habit plane of the precipitate play an important role in increasing the strength of the alloy. They thought that plate-like precipitates grown in the Al plane contributed the most to the strength.¹⁵⁾ SEM-BSE images of the as-extruded alloys are shown in Fig. 1[(d)-(f)]. In the as-extruded alloy, relatively coarse intermetallic compounds with needle shapes, as observed in the as-cast state, were broken down into fine particles and arranged laterally to the extrusion direction owing to the severe deformation during hot extrusion. As the Ni content increased from 0 to 1.0 wt%, the fraction of intermetallic compounds increased to 2.1, 4.9, and 6.6 %, respectively. The intermetallic compound was expected to promote dynamic recrystallization (DRX) during extrusion.

Fig. 2 shows the XRD results for the as-cast and as-extruded Al-1.5 wt%MM-1.5 wt%Sb-xNi ($x = 0, 0.5$ and 1.0 wt%) alloys. The XRD pattern shows a strong peak for the Al phase. Peaks are also observed in the Al₁₁Ce₃, AlSb and Al₃Ni phases. Ni did not show peaks, as represented, which suggests that the nickel was fully consumed. The Al₁₁RE₃ phase is more stable at temperatures below 1000 K as opposed to the Al₄RE isotope, which has been widely studied. Therefore, it can be concluded that while the α -Al and Al₁₁Ce₃ phases are stable present in the Al-rich binary system at low temperatures, the Al₄Ce phase cannot be observed in this experiment [16].

Fig. 3 illustrates the SEM image and EDS analysis of

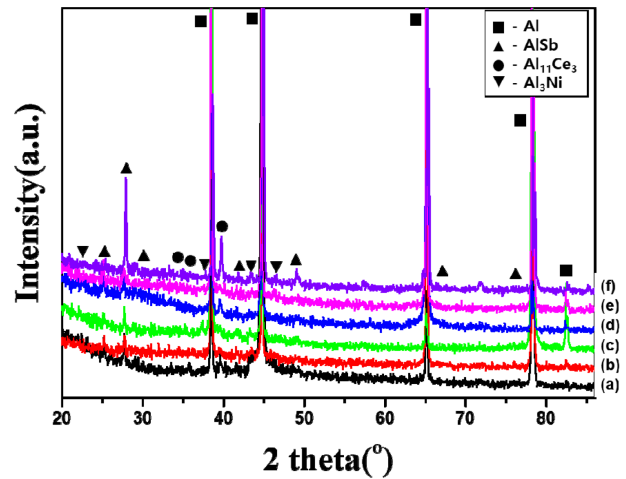


Fig. 2. XRD patterns of the as-cast (a to c) and as-extruded (d to f) Al-1.5 wt%MM-1.5 wt%Sb-xNi alloys [$x = 0$ (a, d), 0.5 (b, e) and 1.0 wt% (c, f)].

the as-cast and as-extruded Al-1.5 wt%MM-1.5 wt%Sb-1.0 wt%Ni alloy. In the alloy Fig. 3[(a) and (b)], small needle-like and lamellar morphology phases [marked (a)] and single polygonal [marked (b)] shapes were observed. Through EDS analysis, lamellar morphology phases and single polygonal shapes were identified as Al₃Ni and AlSb+Al₁₁Ce₃ intermetallic compounds, respectively. The SEM-EDS results are consistent with the XRD results. Earlier literature reveals that the addition of Ni to aluminum alloys would result in the formation of intermetallic like Al₃Ni.

The grain size and texture of the as-extruded Al-1.5 wt%MM-1.5 wt%Sb-xNi alloys were investigated by performing EBSD analysis in a direction parallel to the

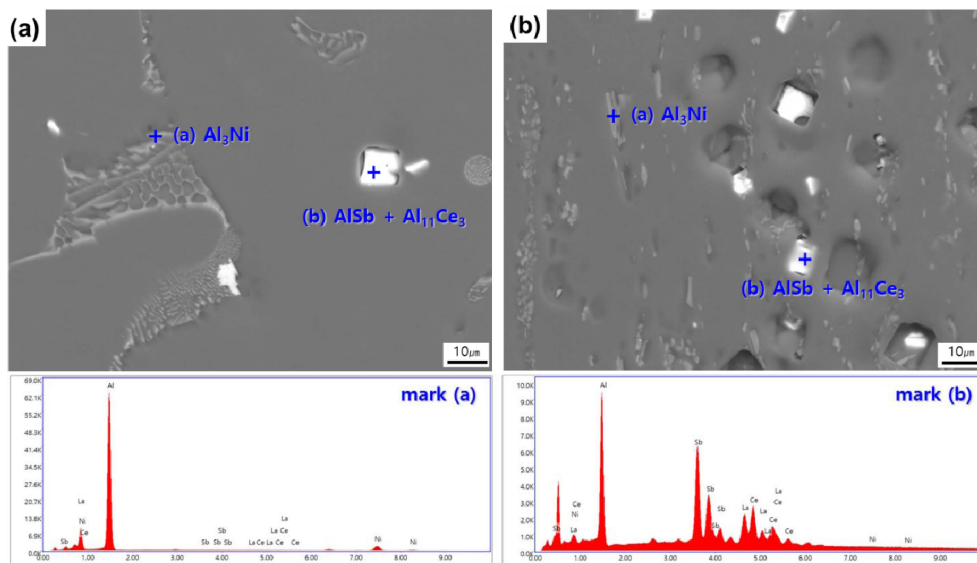


Fig. 3. EDS analysis of the (a) as-cast and (b) as-extruded Al-1.5 wt%MM-1.5 wt%Sb-1.0 wt%Ni alloy.

extrusion direction, as shown in Fig. 4. The average grain size of the as-extruded Al-1.5 wt%MM-1.5 wt%Sb alloy, (a) base metal, (b) add 0.5 wt% Ni, (c) add 1.0 wt% Ni was 1359, 536 and 153 μm , respectively. The larger non-recrystallized grains were elongated in a band shape along the extrusion direction, as shown in Fig. 4(a). On the other hand, the recrystallized grains showed an equiaxed morphology and were finer than the non-recrystallized grains. The increase in the intermetallic compounds increased the driving force for recrystallization and grain refinement. In Figure 4, the low-angle grain boundaries (LGBs) (misorientation of 2 - 15 $^\circ$) and high-angle grain boundaries (HGBs) (misorientation larger than 15 $^\circ$) are shown in red, green, and blue regions, respectively. The non-recrystallized grain regions showed LGBs and recrystallized grain regions were mainly HGB. The high-angle grain boundaries increased to 8, 20 and 34 % as the amount of Ni added increased to 0, 0.5 and 1.0 wt%. The Al_3Ni phase according to the addition of Ni influenced PSN (particle stimulated nucleation) and promoted nucleation for recrystallization.¹⁷⁾ Therefore, it is judged that the microstructure of the extruded material has fine and uniform crystal grains compared to the cast material.

Fig. 5 shows the changes in electrical conductivity of Al-1.5 wt%MM-1.5 wt%Sb-xNi ($x = 0, 0.5$ and 1.0 wt%) alloys according to the as-cast and as-extruded. When Ni alloy is added, the electrical conductivity of the as-extruded was slightly improved compared to that of the as-cast. The electrical conductivity of the as-cast was low owing to the porosity and fine casting defects. As the Ni content increased, the electrical conductivity of the as-extruded Al-MM-Sb alloy decreased by 57.4 % and 57.1 % International Annealed Copper Standard (IACS). The

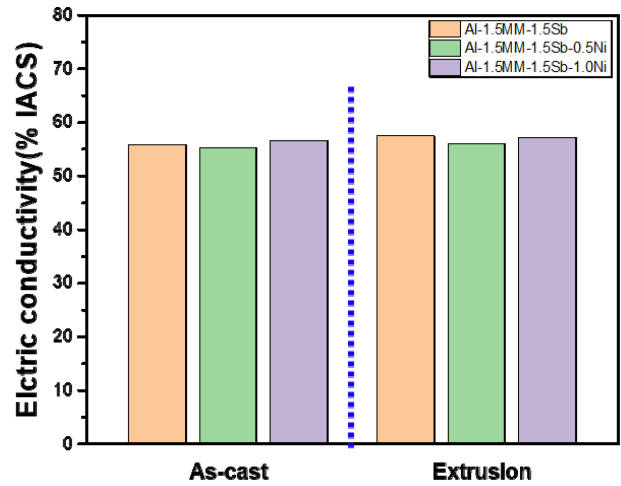


Fig. 5. Electric conductivity of the as-cast and as-extruded Al-1.5 wt%MM-1.5 wt%Sb-xNi alloys.

decrease in electrical conductivity is due to the addition of Ni. The added Ni had a solid solution in the a-Al matrix and affected the electrical conductivity of the alloy. Alloying elements affect the Al alloys electrical conductivity in several ways. As the amount of alloying elements increases, the Al solid solubility was exceeded and precipitates or intermetallic compounds of different morphologies are formed. Due to the addition of Ni, the increase in the grain boundary phase lowered the electrical conductivity, and in the case of the extruded material, the distribution of the grain boundary precipitated phase was improved and the electrical conductivity was slightly increased.

Fig. 6 show the tensile properties of the as-extruded Al-1.5 wt%MM-1.5 wt%Sb alloys with increasing Ni contents. As the Ni alloy increased from 0 to 1.0 wt%,

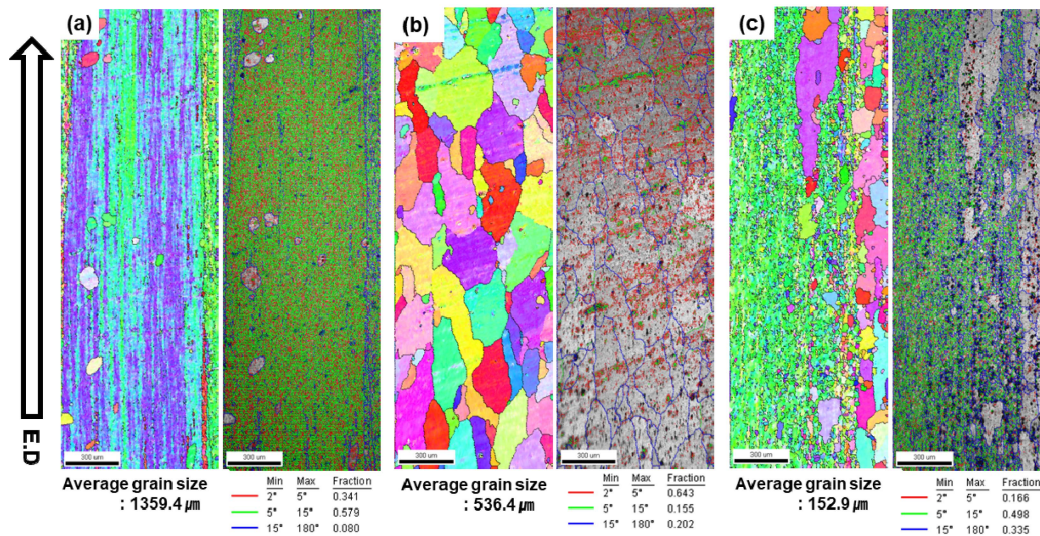


Fig. 4. EBSD analysis (IPF image, IQ map) of the as-extruded (a) Al-1.5 wt%MM-1.5 wt%Sb, (b) Al-1.5 wt%MM-1.5 wt%Sb-0.5 wt%Ni, (c) Al-1.5 wt%MM-1.5 wt%Sb-1.0 wt%Ni alloys.

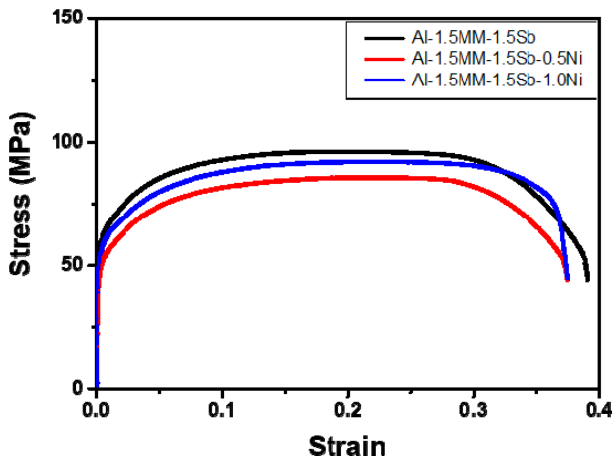


Fig. 6. Tensile stress–strain curves of the as-extruded Al-1.5 wt%MM-1.5 wt%Sb-xNi alloys at room temperature.

the ultimate tensile strength decreased from 96.1 MPa to 92.0 MPa, and the elongation decreased from 39.1 % to 37.5 %. The uniform elongation was 20.7 %, 22.6 %, and 23.5 %, and the work hardening index n -value was 0.1468, 0.2110 and 0.2052, which was the highest at Al-1.5 wt% MM-1.5 wt%Sb-0.5 wt%Ni alloy. Uniform strain during tensile test can be used effectively as a measure of n -value, which relates to ductility. The addition of Ni to the Al alloy had an effect on improving the recrystallization properties, but did not significantly affect the tensile properties and conductivity. The Al₃Ni particles improved hardness and wear resistance, but the literature did not report significant improvement in the tensile behavior of aluminum alloys.¹⁸⁾

4. Conclusion

In this study, the microstructure and mechanical properties of cast and extruded Al-1.5wt%MM-1.5wt%Sb-xNi ($x = 0, 0.5$ and 1.0 wt%) alloy were comparatively investigated by SEM, EBSD and conducting tensile tests. With an increase in the Ni content the average grain size significantly decreased from 1359 to 153 μm and the HGB fraction increased from 8 to 34 %. In the case of the alloys, the addition of Ni affects PSN and promotes nucleation for recrystallization. The electrical conductivity of Al-MM-Sb alloy added with Ni was 57.4 and 57.1 %IACS, which was almost similar. The addition of Ni to the Al alloy had an effect on improving the recrystallization properties, but did not significantly affect the tensile properties and conductivity.

Acknowledgments

This study has been conducted with the support of the Korea Institute of Industrial Technology as “Development of Core Technologies for a Smart Mobility (kitech JA-21-0005)”.

References

1. H. Jiang, S. Li, Q. Zheng, L. Zhang, J. He, Y. Song, C. Deng and J. Zhao, *Mater. Des.*, **195**, 108991 (2020).
2. S.-S. Na, Y.-H. Kim, H.-T. Son and S.-H. Lee, *Korean J. Mater. Res.*, **30**, 542 (2020).
3. D. Li, C. Cui, X. Wang, Q. Wang, C. Chen and S. Liu, *Mater. Des.*, **90**, 820 (2016).
4. A. E. Medvedev, M. Y. Murashkin, N. A. Enikeev, R. Z. Valiev, P. D. Hodgson and R. Lapovok, *J. Alloys Compd.*, **745**, 696 (2018).
5. C.-G. Jung, U. Hiroshi, H.-T. Son and S.-H. Lee, *Korean J. Mater. Res.*, **27**, 597 (2017).
6. M. Y. Murashkin, I. Sabirov, A. E. Medvedev, N. A. Enikeev, W. Lefebvre, R. Z. Valiev and X. Sauvage, *Mater. Des.*, **90**, 433 (2016).
7. Q. Zheng, L. Zhang, H. Jiang, J. Zhao and J. He, *J. Mater. Sci. Tech.*, **47**, 142 (2020).
8. A. A. Mogucheva, D. V. Zyabkin and R. O. Kaibyshev, *Met. Sci. Heat Treat.*, **53**, 450 (2012).
9. S. S. Nayak, M. Wollgarten, J. Banhart, S. K. Pabi and B. S. Murty, *Mater. Sci. Eng., A*, **527**, 2370 (2010).
10. W. Ding, X. Zhao, T. Chen, H. Zhang, X. Liu, Y. Cheng and D. Lei, *J. Alloys Compd.*, **830**, 154685 (2020).
11. Z. Mao, D. N. Seidman and C. Wolverton, *Acta Mater.*, **59**, 3659 (2011).
12. C. Li, C. Wang, Z.-Z. Yang, P.-K. Ma, M.-W. Ren and H.-Y. Wang, *J. Alloys Compd.*, **869**, 159304 (2021).
13. R. Akhil, O. P. Nath and S. Arul, *Mater. Today: Proc.*, **24**, 1042 (2020).
14. L. Pan, S. Zhang, Y. Yang, N. Gupta, C. Yang, Y. Zhao and Z. Hu, *Metall. Mater. Trans. A*, **51**, 214 (2020).
15. B. Jiang, H. Wang, D. Yi, Y. Tian, F. Shen, B. Wang, H. Liu and Z. Hu, *Mater. Charact.*, **162**, 110184 (2020).
16. Z. Cao, G. Kong, C. Che, Y. Wang and H. Peng, *J. Rare Earths*, **35**, 1022 (2017).
17. J. D. Robson, D. T. Henry and B. Davis, *Acta Mater.*, **57**, 2739 (2009).
18. M. Balakrishnan, I. Dinaharan, K. Kalaiselvan and R. Palanivel, *J. Mater. Res. Technol.*, **9**, 4356 (2020).

Author Information

Hyo-Sang Yoo

Korea Institute of Industrial Technology, Researcher

Yong-Ho Kim

Korea Institute of Industrial Technology, Researcher

Cheol-Woo Kim

Korea Institute of Industrial Technology, Researcher

Se-Weon Choi

Korea Institute of Industrial Technology, Principal Researcher

Hyeon-Taek Son

Korea Institute of Industrial Technology, Principal Researcher